UNIVERSITY OF CALIFORNIA, SAN DIEGO

MicroRNA-101 Regulates NKCC1, Kif1a, and Ank2 to Fine-Tune the Formation of Proper Neural Networks

A thesis submitted in partial satisfaction of the

requirements for the degree Master of Science

in

Biology

by

Jerry Chia Ye Liu

Committee in Charge:

Professor Darwin K. Berg, Chair
Professor Nicholas C. Spitzer, Co-Chair
Professor Gulcin Pekkurnaz

2017

The thesis of Jerry Chia Ye Liu is approved, and it is acceptable in quality and form for publication on microfilm and electronically:

_____

_____

Co-Chair

_____

Chair

University of California, San Diego

2017

DEDICATION

I dedicate my Thesis to my parents, John and Emma, who taught me the importance of tenacity in success.

EPIGRAPH

“Do not fear failure but rather fear not trying.”

Roy T. Bennett, The Light in the Heart

TABLE OF CONTENTS

Signature Page iii

Dedication iv

Epigraph v

Table of Contents vi

List of Figures vii

List of Supplemental Figures viii

Abstract of Thesis ix

Chapter I: Introduction 1

Chapter II: Inhibition of miRNA-101 and miRNA-218 leads to hyperexcitable networks 6

Chapter III: MiRNA-101 can silence relevant targets through degradation 10

Chapter IV: MiRNA-101 regulates dendritic growth 14

Chapter V: MiRNA-101 constrains the formation of glutamatergic synapses 17

Chapter VI: Discussion 20

Appendix I: Acknowledgements 23

Appendix II: Materials and Methods 24

Bibliography 31

LIST OF FIGURES

Figure 1. Inhibition of MiRNA-218 Leads to Increased Numbers of Synchronized Events 8

Figure 2. Validation of MiRNA-101 and MiRNA-218 Predicted Targets Using Sensor Technology..... 13

Figure 3. MiRNA-101 Regulates NKCC1 to Restrain Dendritic Development. ... 16

Figure 4. MiRNA-101 Regulates Ank2 and Kif1a to Fine-Tune the Formation of Presynaptic Puncta and Spinogenesis 19

LIST OF SUPPLEMENTAL FIGURES

Supplemental Figure 1. Inhibition of MiRNA-101 Leads to Increased Synchronized and Total Events 9

Supplemental Figure 2. MiRNA-101 and –218 qPCR Results and Candidate Targets. 12

ABSTRACT OF THE THESIS

MicroRNA-101 Regulates NKCC1, Kif1a, and Ank2 to Fine-Tune the Formation of Proper Neural Networks

by

Jerry Chia Ye Liu

Master of Science in Biology

University of California, San Diego, 2017

Professor Darwin Berg, Chair

Professor Nicholas C. Spitzer, Co-Chair

MicroRNAs (miRNAs) are post-transcriptional regulators that coordinate the execution of developmental programs across all cell types. Current methods for identifying targets of miRNAs are initially theoretical. It is, therefore, essential

to carry out in-vivo experiments to validate those relationships. MiRNA-101 is highly expressed in the brain and has predicted targets that are influential in neural development. Using sensor technology, we were able to show that miRNA-101 represses the expression of NKCC1, Kif1a, and Ank2. Furthermore, interference of miRNA-101 and its target NKCC1, led to increased dendritic growth, while simultaneous protection of Kif1a and Ank2 gave rise to excessive glutamatergic synapse formation. These findings verify the relationship between miRNA-101 and some of its targets, and suggest sites for therapeutic intervention for treatment of diseases that arise from excessive early network growth.

Chapter I: Introduction

MicroRNAs (miRNAs) are a family of 20 to 30 nucleotide long non-coding RNAs that associate with Argonaute (AGO) family proteins and are categorized as small RNAs (Bartel 2004). They are highly conserved short strands of noncoding RNA that serve as post-transcriptional regulators of gene expression (Huntzinger and Izaurralde 2011). Although small in size, each miRNA can potentially manage upwards of hundreds of different targets (Huntzinger and Izaurralde 2011).

The biogenesis and maturation of miRNAs have been well studied. MiRNA development begins in the nucleus when RNA polymerase II transcribes primary miRNAs (pri-miRNAs) from miRNA genes and introns of coding transcripts (Lee et al., 2002). Newly transcribed pri-miRNAs are 33-35 base-pairs long with a hairpin structure containing a terminal loop that is flanked by single-stranded RNA segments at both its 5' and 3' ends (Ha and Kim 2014). The development of pri-miRNAs into mature miRNAs is initiated by a Microprocessor containing Drosha and its cofactor DGCR8 (Han et al., 2004).

Drosha is a 160kDa RNAse III-type endonuclease that is localized predominantly within the nucleus (Wu et al., 2000). Both the amino and carboxyl terminus of Drosha play critical roles in allowing Drosha to properly function within physiological environments. Phosphorylation at either Serine 300 or Serine 302 within the amino-terminal end of Drosha initiates its nuclear-localization process (Tang et al., 2010). The carboxyl end of Drosha contains both tandem RNase III domains and a dsRNA-binding domain (Ha and Kim 2014). The RNase

III domains cooperate with each other to create a processing center that possesses two catalytic dsRNA cleavage sites (Han et al., 2004). Proper operation of these catalytic sites is dependent on Drosha joining with the cofactor DiGeorge syndrome critical region 8 (DGCR8) (Han et al., 2004). Combined, DGCR8 and Drosha form the bulk of the Micropressor unit, allowing its cleavage sites to forge short, 2 to 3 nucleotides, overhangs at the stem of local hairpin structures embedded within pri-mRNAs (Winter et al., 2009). The action of the Micropressor unit releases the hairpin structures, transforming them into pre-miRNAs (Lee et al., 2003).

Pre-miRNAs contain a single-stranded terminal loop attached to a double stranded RNA (dsRNA) (Winter et al., 2009). The separation of the terminal loop from the double-stranded miRNA (dsmiRNA) undergoes a process similar to that of the genesis of pre-miRNAs by Drosha. Newly synthesized pre-miRNAs are exported into the cytoplasm by nuclear export factor exportin 5 where Dicer, another RNAse III enzyme, cleaves the terminal loop from the hairpin structure of pre-miRNA forming a small RNA duplex of 21 to 23 nucleotides in length (Bernstein et al., 2001; Knight and Bass 2001).

In Dicer-directed cleavage, the RNAse III domains within the Carboxyl terminus of Dicer form intramolecular dimerization leading to the activation of a catalytic cleavage site (Zhang et al., 2004). Dicer's N-Terminal domain is responsible for identifying the single-stranded terminal loop within the stem-loop pre-miRNA (Tsutsumi et al., 2011). Verification of pre-miRNA paves the way for binding domains within Dicer to bind to the termini of pre-miRNA, bringing pre-

miRNA restriction sites to Dicer's cleavage centers (Park et al., 2011). Removal of the terminal loop is followed by a two-step RNA-induced silencing complex (RISC) assembly process (Kawamata and Tomari 2010). The first step involves loading the newly refined miRNA duplex, containing a 'passenger' and a 'guide' strand, onto an AGO protein (Kawamata and Tomari 2010). The second step involves removal of the 'passenger' strand from the loaded miRNA duplex (Kawamata and Tomari 2010).

Matured mammalian RISC contains AGO, a deadenylase complex, decapping factors, and a single-stranded guide miRNA to repress the translation of its targets. (Gregory et al., 2005; Huntzinger and Izaurralde 2011). The loaded 'guide' miRNA predominantly forms partial to fully complementary base-pairing with 'seed sequences' within 3' untranslated regions of its targets to bring RISC and its RNA destabilization complexes into close proximity of its targets to degrade them (Yekta et al., 2004). However in more rare cases, 'seed sequences' may fall within mRNA coding domains (Duursma et al., 2008). In addition to decay, miRNA-RISC also silences targets through translational repression. Through the repression system, target mRNAs remain whole but their translation is constrained by RISC interfering with translational machineries from reading the scripts (Iwakawa and Tomari 2015).

Strong links have been established between miRNAs and diseases of the nervous system. Tourette's syndrome, a neuropsychiatric disorder, is found to be associated with mutations in the miRNA-189 seed sequence of SLITRK1, leading to the overexpression of the gene (Abelson et al., 2005). Loss of the key players

FMRP and DGCR8 in the miRNA processing pathway are, respectively, found to be associated with Fragile X syndrome and DiGeorge syndrome; both conditions share characteristics of cognitive impairment (Digilio et al., 2005; Jin et al., 2004). Neurodevelopmental disorders associated with miRNAs are not limited to their loss of function. Seizure-associated cognitive disorders such as Down syndrome and epilepsy are both linked to overexpression of miRNAs (Kuhn et al., 2010; Elton et al., 2010).

Beyond their connection to neurological diseases, miRNAs also act as positive regulators to promote neural maturation, connectivity, and plasticity (Cuellar et al., 2008; Davis et al., 2008; Kawase-Koga et al., 2009). MiRNAs can also act as negative regulators, serving as brakes to delay each of these steps (Rajasethupathy et al., 2009; Smrt et al., 2010). Combined, the positive and negative regulatory functions of miRNAs fine-tune neurodevelopment to ensure that the process is balanced and controlled.

Although miRNAs are proven to be critical in the execution of developmental programs, there still exists a vast number of miRNAs with unknown function. The work carried out in our lab examines the contribution of miRNAs to neural network formation. We use a molecular approach to characterize miRNAs that are involved in neurodevelopment. One consequence is that the results may shed light on the etiology of diseases that arise from improper early brain development.

There is an immense number of miRNAs in the brain. In order to narrow our search for miRNAs that play a role in neurodevelopment, we pursued

miRNAs that are abundantly expressed in the brain, upregulated during a critical developmental window, and have predicted targets that are involved in neuronal function. Using results obtained from RNAseq, HITS-CLIP, and TARGETSCAN, we found that miRNA-101, -136, and -218 were top candidates for further experimentation. To assess the effects that these miRNAs have in neurodevelopment, we employed RNA antagonists to individually prevent each candidate miRNA from regulating its specific targets. Alternatively, we used antagonists to protect individual targets from being regulated by a given miRNA. Our findings identify miRNA-101 as a key player in directly regulating NKCC1 to limit dendritic growth, and Kif1a and Ank2 to prevent excessive glutamatergic synapse formation during early brain development. In addition, we find that miRNA-218 appears to limit synchronous activity, possibly through indirect targeting of Kif21b and Syt13.

Chapter II: Inhibition of miRNA-101 and miRNA-218 leads to hyperexcitable networks

Early postnatal development can be seen as having two phases: an early phase where a coarse network is laid out, and a later period where synapses are pruned to leave behind a refined neural network (Blankenship and Feller 2010). Early phase development is marked by two distinct patterns of spontaneous activity. In rodents, during the period between a few days before to five days after birth, the dominant spontaneous activity pattern is synchronous plateau assemblies (SPAs) (Crepel et al., 2007). Following postnatal day five, giant depolarizing potentials (GDPs) become the prevalent spontaneous activity pattern. During this window, neighboring neurons frequently and simultaneously initiate SPAs and GDPs to contribute to waves of neural activity to produce synchronized events (SEs) (Katz and Shatz 1996).

Spontaneous activity and SEs drive the development of the coarse networks observed in early development (Blankenship and Feller 2010; Ben-Ari 2002). To determine whether miRNA-101, -136, and -218 possess any role in generating spontaneous activity and SEs, and in turn, paving coarse networks, localized transient inhibition was performed via separate injections of synthetic antagonists (a.101.F, a.136.F, and a.218.F) for each miRNA into the dorsal hippocampus of postnatal day 2 pups (P2). These antagonists are locked nucleic acids (LNAs) that are designed to have target specificity, to readily enter cells, to be resistant to degradation, and to contain a fluorescent marker to track them. LNA injections, where the sequences were designed to not recognize any

miRNAs, were employed as controls (a.Ctrl.F). P2 was chosen because it is within the critical developmental window preceding the establishment of adult neural networks (Ben-Ari 2001). Six days post-injection of antagonists and prior to the onset of decreased antagonist efficacy, recordings of calcium activity were made on acute hippocampal slices treated with fluo-4, a calcium dye (Paredes et al., 2008).

Calcium channels are typically open between the peak and falling phase of neuronal action potentials. Thus calcium flux serves as a good indicator of neuronal activity (Bean 2007). We found that hippocampal slices of animals treated with a.101.F or a.218.F had significantly increased numbers of synchronized events, that is, periods when at least 15% of the neurons participating in SPAs or GDPs exhibited activity simultaneously (Figures 1A-C and S1B). Furthermore, when analyzing the total number of events, a.101.F conditions led to increases in the amount of activity, regardless if they were part of synchronized events (Figure S1A). Conditions with a.136.F did not lead to any changes in calcium activity when compared to control (Figures 1B-1C). The lack of an effect on calcium activity in animals with inhibited miRNA-136 suggests that it is not involved in regulating calcium activity. Accordingly, we focused on miRNA-101 and miRNA-218.

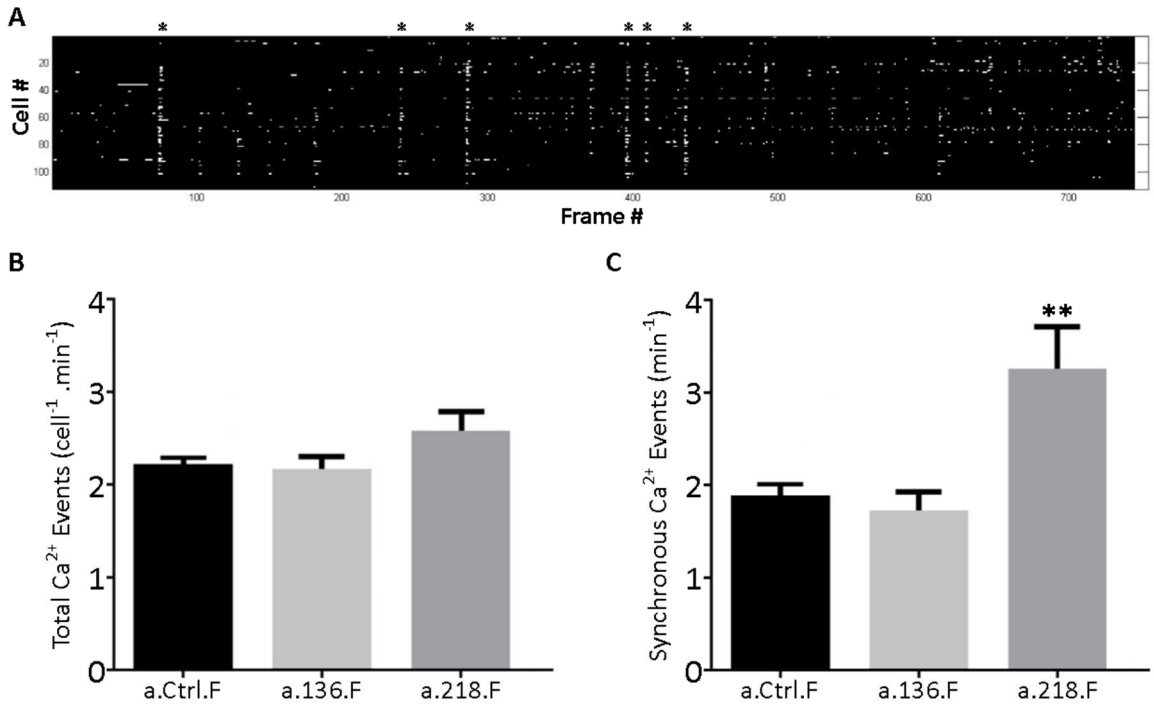

Figure 1. Inhibition of miRNA-218 Leads to Increased Numbers of Synchronized Events. (A) The top panel contains an example of a raster plot that depicts calcium activity of neurons captured during calcium imaging. Each row represents an individual neuron, and each column represents a movie frame. White dots represent the frame in which its corresponding neuron showed activity. The asterisks denote the frames that captured synchronous Ca^{2+} events. (B-C) When compared to control a.Ctrl.F, no changes in total Ca^{2+} events were observed in a.136.F and a.218.F conditions, while an increase in synchronous Ca^{2+} events was observed in the a.218.F condition.

Bar graphs: mean $\pm$ SEM, one-way ANOVA with Tukey's multiple comparison test; *$p < 0.05$, **$p < 0.01$, ***$p < 0.001$.

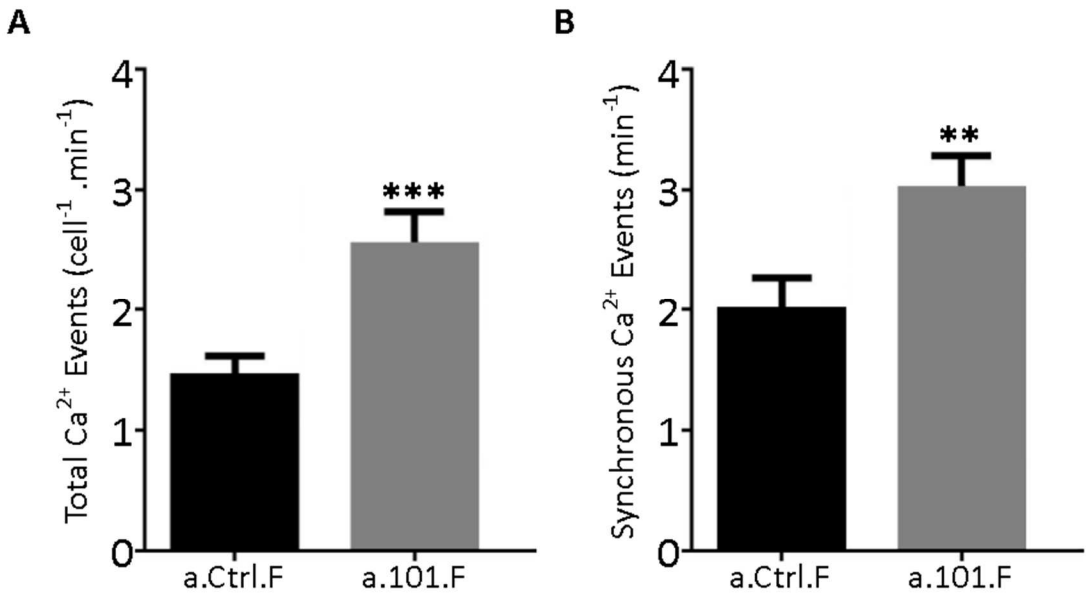

Supplemental Figure 1. Inhibition of MiRNA-101 Leads to Increased Synchronized and Total Events. (A-B) Animals injected with a.101.F showed increases in both total and synchronous Ca^{2+} events.

Bar graphs: mean ± SEM, one-way ANOVA with Tukey's multiple comparison test; *p < 0.05, **p <0.01, ***p < 0.001.

Chapter III: MiRNA-101 can silence relevant targets through degradation

Candidate targets for miRNA-101 and -218 were compiled using TARGETSCAN. The list was narrowed by selecting candidates that appeared in mouse and human cortex HITS-CLIP databases, and that appeared likely to contribute to the increased activity associated with hippocampal network formation (Boudreau et al., 2014; Chi et al., 2009) (Figures S2C-D). HITS-CLIP is a process that combines **hi**gh **t**hroughput **s**equencing with **c**ross**l**inking **i**mmuno**p**recipitation to provide a list of candidates that are associated with Ago-miRNA-mRNA complexes (Darnell 2010).

Prior qPCR experiments conducted in the lab have showed that miRNA-101 and -218 are upregulated in early brain development (Lippi et al., 2016)**.** Based on those findings, qPCR experiments were conducted on candidate mRNAs while in the presence of a.101.F or a.218.F. To do so, a.101.F and a.218.F were separately injected into P2 animals. Hippocampal tissue samples used for qPCR experiments were extracted from P7 animals for a.101.F conditions and from P8 animals for a.218.F conditions. qPCR results showed an increase in expression levels of the targets NKCC1, Kif1a, and Ank2 for miRNA-101, and Kif21b and Syt13 for miRNA-218 (Figures S2A-B).

To determine the mechanism by which miRNA-101 and -218 silence these targets, sensor assays were employed. These assays were carried out using plasmids containing a green fluorescent protein (GFP) gene driven by a cytomegalovirus promoter (CMV) and a far red fluorescent protein (RFP_{670}) gene driven by a CAG promoter (Figure 2A). For experimental conditions, we cloned

truncated versions of the 3' UTR, containing wild-type or mutant MREs, of the putative miRNA targets downstream of RFP_{670}. Sequences were compared to online databases to ensure that MREs for other highly neuronally expressed miRNAs were not introduced. Completed sensor plasmids for miRNA-101 and -218 targets were packaged into lentiviruses and injected into the hippocampus of P2 animals.

The results from the experiment showed lower RFP_{670} to GFP ratios in target sensors of miRNA-101 when compared to mutated conditions (Figure 2B-C). This finding, in conjunction with upregulated mRNA data found via qPCR, demonstrates that miRNA-101 silences NKCC1, Kif1a, and Syt13 by directly interacting with MREs within their 3' UTR, leading them to being degraded. MiRNA-218 targets, when compared to mutated conditions, showed no change in RFP_{670} to GFP ratios (Figure 2D). This finding, while taking into account the qPCR results, suggests that miRNA-218 influences the translation of Kif1a and Syt13 through other means (see Discussion).

A

MiRNA-101 (P7)					
Target	a.Ctrl	S.E.M.	a.101.F	S.E.M.	P-Value
NKCC1	1.00	0.04	1.48	0.00	0.001
Kif1a	1.00	0.01	1.50	0.12	0.014
Ank2	1.00	0.08	1.74	0.29	0.049

B

MiRNA-218 (P8)					
Target	a.Ctrl	S.E.M.	a.218.F	S.E.M.	P-Value
Kif21b	1.00	0.03	1.18	0.05	0.011
Syt13	1.00	0.07	1.19	0.04	0.023

C

Target	Function
NKCC1	NKCC1 is a membrane protein that aids in the active transport of sodium, potassium, and chloride ions into and out of cells (Haas M., 1994). Over the course of development, NKCC1 expression drops to contribute to lower endogenous Cl^- concentration resulting in GABA switching from an inhibitory to excitatory neurotransmitter (Tyzio et al., 2006).
Kif1a	Kif1a is a motor protein that falls in the kinesin-3 family and is responsible in transporting synaptic vesicles along axons (Hirokawa et al., 2010). The overexpression of Kif1a has been found to promote synaptogenesis via the formation of presynaptic boutons (Kondo et al., 2012).
Ank2	Ank2 is part of a family of adaptor proteins that contribute to structural stability of plasma membranes (Bennett et al., 2013). Within neurodevelopment, Ank2 has been found to promote axonal growth and maintain synaptic stability at the presynaptic terminal (Bulat et al., 2014; Lorenzo et al., 2014).

D

Target	Function
Kif21b	Another kinesin-3 family member, Kif21b has been implicated with promoting dendritic arborization and spine development (Muhia 2014).
Syt13	The Ca^{2+} domain of synaptotagmins act as Ca^{2+} sensors of exocytosis in neuronal cells (Chen et al., 2017). Syt13 lacks the Ca^{2+} domain and it has been speculated to be involved with constitutive vesicle transport rather than Ca^{2+} regulated exocytosis (Fukuda et al., 2001).

Supplemental Figure 2. MiRNA-101 and –218 qPCR Results and Candidate Targets. (A-B) qPCR was used to quantify target mRNA levels while in the presence of inhibited miRNA function. Animals were injected at P2, and qPCR was conducted on hippocampal tissue samples of P7 mice for miRNA-101 conditions and P8 mice for miRNA-218 conditions. Values are expressed as mean ± SEM. Experimental conditions were normalized to a.Ctrl animals. P values were determined using Student's t test. Candidate targets and their corresponding functions are respectively listed in panels C and D for miRNA-101 and –218.

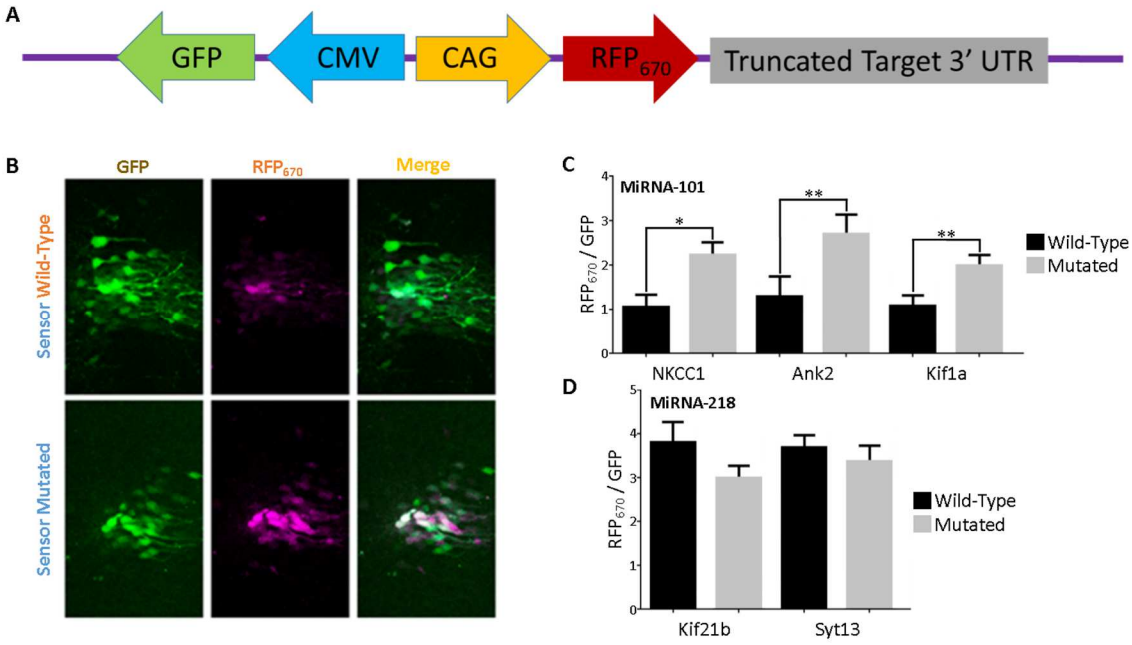

Figure 2. Validation of MiRNA-101 and MiRNA-218 Predicted Targets Using Sensor Technology. (A) The top panel contains the scheme of the sensor plasmids that were used to determine the mechanism by which miRNA-101 and -218 silence their targets. (B) Hippocampal neurons from animals injected with NKCC1 sensors containing wild-type MREs were compared to those injected with mutated MREs. GFP was used to normalize RFP_{670} fluorescent intensity. (C) A decrease in RFP_{670}/GFP was observed between wild-type and mutated conditions for miRNA-101 targets. (D) No differences were observed in miRNA-218 conditions.

Bar graphs: mean $\pm$ SEM, Student's t test; *p < 0.05, **p <0.01.

Chapter IV: MiRNA-101 regulates dendritic growth

The finding that miRNA-101 targets the chloride transporter NKCC1 raises the possibility that it influences neural network formation by promoting the transition in signaling from excitatory to inhibitory seen for the transmitter γ-aminobutric acid (GABA). While GABA is the primary inhibitory neurotransmitter in the adult brain, activation of $GABA_A$ receptors in neonates leads to the excitation of many neurons. The foundation for the transition of excitatory to inhibitory GABA is due in part to high early expression of NKCC1. NKCC1, is a membrane bound Na^+-K^+-$2Cl^-$ cotransporter that is tasked with bringing chloride into cells. Its action produces a depolarized Cl^- equilibrium potential, causing efflux of chloride ions during GABAergic signaling and leading to depolarization of neurons (Yamada et al., 2004). During the second week of postnatal life in rodents, NKCC1 expression levels decline while the chloride extruding K^+-Cl^- cotransporter, KCC2, increases to establish the chloride gradient found in mature neurons (Rivera et al., 1999; Tyzio et al., 2006).

Excitatory GABA has been implicated as a key component behind GDPs, which are thought to play a crucial role in the maturation of neuronal circuits (Leinekugel et al., 2002). Premature switching from an excitatory to inhibitory role has been shown to reduce dendritic length and branch numbers (Cancedda et al., 2007). Together, with the increased calcium activity levels observed in the presence of a-101.F, we hypothesized that protecting NKCC1 from miRNA-101 repression would lead to more elaborate dendritic complexity, thereby revealing the regulatory role that miRNA-101 normally plays.

In order to test this hypothesis, we co-injected target-site blockers (TSBs), along with pseudorabies virus encoding eGFP, into the hippocampus of P2 animals. TSBs are LNAs that are complementary to a single MRE on a specific target, thus selectively protecting that target from miRNA repression and leaving all other targets still repressed. Pseudorabies virus was used to provide sparse labeling of neurons. Images of CA1 and CA3 proximal pyramidal neurons were taken at P8 (Figure 3A). In the presence of NKCC1-TSB alone, the length of primary dendrites increased in CA1, and increased for both primary and secondary branches in CA3 (Figure 3B-C). These results demonstrate that miRNA-101 regulates NKCC1 to contribute to the orderly switch of GABA, and indirectly regulates dendritic growth.

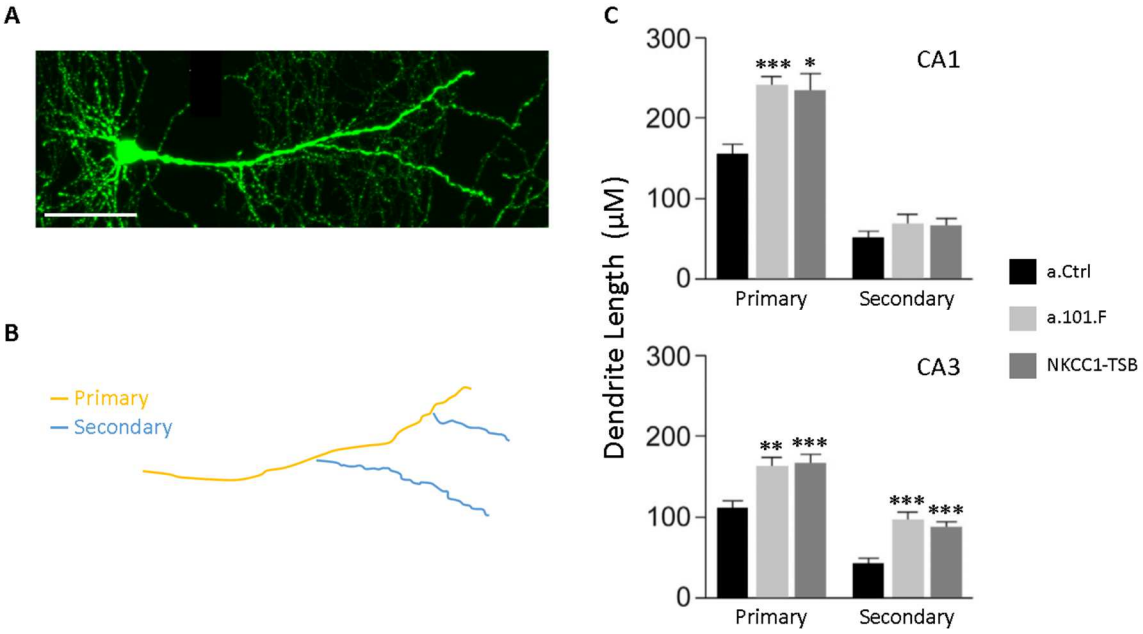

Figure 3. MiRNA-101 Regulates NKCC1 to Restrain Dendritic Development. (A) Sparse labeling of hippocampal neurons was achieved through the use of rabies virus expressing EGFP (scale bar 50 μm). (B) Dendritic tracings were made using NeuronJ to measure dendritic lengths. (C) Interference with miRNA-101 led to longer primary and secondary dendrites in CA3 neurons and longer primary dendrites in CA1 neurons. Protecting NKCC1 from miRNA-101 phenocopied these results.

Chapter V: MiRNA-101 constrains the formation of glutamatergic synapses

Kif1a and Ank2, two additional miRNA-101 targets, have been linked to glutamatergic synapse formation. Kif1a is a member of a family of kinesin motors that are transport synaptic vesicle proteins, while Ank2 is a broadly expressed adaptor protein that mediates the attachment of integral membrane proteins (Hirokawa et al., 2009; Moler et al., 2002). Overexpression of Kif1a has been shown to increase the number of presynaptic boutons, and Ank2 has been implicated in synapse stabilization (Bulat et al., 2014; Kondo et al., 2012). These findings led us to the hypothesis that release of Kif1a and Ank2 from miRNA-101 inhibition would increase the number of glutamatergic synapses. To test this hypothesis, we examined glutamate transporter (VGluT1) levels and dendritic spine numbers in animals injected with a.Ctrl versus a.101.F, NKCC1 TSB, or with combined injections of NKCC1, Kif1a, and Ank2 TSBs. Injections were made into the hippocampus of P2 animals, and analysis was performed at P11 or P15.

Analysis of presynaptic glutamatergic synapses was done within the striatum radiatum of hippocampal slices that were immunostained for VGluT1 (Figure 4A). VGluT1 is a vesicular glutamate transporter that can be used as a marker for presynaptic glutamatergic synapses (Takamori et al., 2006). The striatum radiatum contains a large presence of associational and commissural connections, making it an ideal location for visualizing glutamatergic synapses. No difference in VGluT1 puncta density was seen between P15 animals injected with a.Ctrl and those injected with NKCC1 TSB (Figure 4B-C). P15 animals

injected with combined TSBs for NKCC1, KIF1a, and Ank2 phenocopied the increase in puncta density seen in animals receiving a.101.F (Figure 4C).

Dendritic spines are small protrusions that represent postsynaptic sites of excitatory synapses (Hering and Sheng, 2001). Analysis of dendritic spines were made on CA1 and CA3 pyramidal neurons of P11 animals. Pseudorabies virus encoding eGFP was used to visualize cells. Dendritic protrusions were separated into the classifications “mushroom”, “stubby”, “thin”, and “filopodia” (Hering and Sheng 2001; Kanjhan et al., 2016) (Figure 4D). No difference in the number of protrusions was seen between animals treated with a.Ctrl and those with NKCC1 TSB (Figure 4F). Animals treated with combined TSBs for NKCC1, KIF1a, and Ank2 phenocopied the increase in protrusions seen in those with a.101.F treatment (Figure 4E-F). Of the major dendritic protrusion classes, “mushroom” showed the most pronounced increase (Figure 4G). Interestingly, “mushroom” spines have been shown to represent mature glutamatergic synapses (Chen and Sabatini 2012). Combined with increased VGluT1 puncta density, these findings suggest that miRNA-101 regulates KIF1a and Ank2 to limit the density glutamatergic synapses.

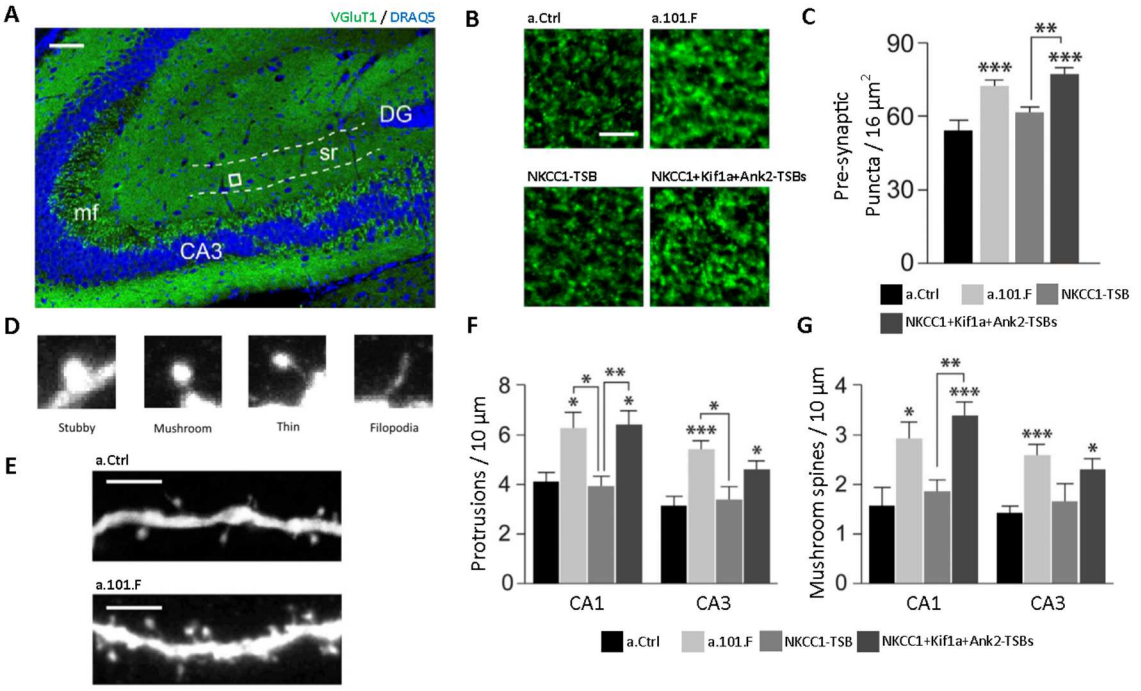

Figure 4. MiRNA-101 Regulates Ank2 and Kif1a to Fine-Tune the Formation of Presynaptic Puncta and Spinogenesis. (A) Immunostaining for presynaptic VGlut1 was done in the stratum radiatum (sr) (scale bar 50 µm). (E-F) Protection of NKCC1 alone was insufficient to phenocopy pre-synaptic VGlut1 puncta levels. (D) Separate counts of stubby, mushroom, and thin spines were made to quantify the effects of miRNA-101 on spinogenesis. (E) Spines were captured through confocal imaging (scale bar 5 µm). (F-G) Protection of Kif1 and Ank2 in addition to NKCC1 was necessary to phenocopy increases of dendritic protrusions induced by a.101.F.

Bar graphs: mean ± SEM, one-way ANOVA with Tukey's multiple comparison test; *p < 0.05, **p <0.01, ***p < 0.001.

Chapter VI: Discussion

While advancements in bioinformatics and molecular biology paved the way for tools such as TARGETSCAN and HITS-CLIP to rapidly predict miRNA-mRNA target interactions, these predicted targets are often times incorrect, and thus, there is still a need to experimentally validate such interactions. This study aimed to verify miRNAs that have predicted roles in neurodevelopment, simultaneously uncover those roles, and in turn produce a better understanding of the etiology behind diseases of the brain. We used LNAs to demonstrate that miRNA-101 and -218 are active in early phase hippocampal development to prevent the construction of hyperexcitable networks. Furthermore, we employed sensor experiments and TSBs to show that miRNA-101 directly targets NKCC1, Kif1a, and Ank2 to constrain dendritic complexity.

The mechanism by which miRNAs suppress their targets is strongly contested. Evidence suggests that miRNAs either degrade their targets or block them from translation while leaving the transcripts intact (Duursma et al., 2008; Yekta et al., 2004). Experiments employing qPCR showed an increase in NKCC1, Kif1a, and Ank2 mRNA levels for miRNA-101, and Syt13 and Kif21b for miRNA-218 while in the presence of antagonists. These findings suggest that miRNA-101 and -218 degrade their transcripts. Sensor experiments designed to validate miRNA-MRE interactions corroborated qPCR results that interaction between miRNA-101 and target MREs led to degradation of the target transcript. In contrast, results from experiments with miRNA-218 antagonists failed to confirm that miRNA-218 directed target degradation, despite the qPCR findings.

These conflicting sets of results for miRNA-218 suggest that Kif21b and Syt13 may be indirectly targeted by miRNA-218, rather than being directly degraded.

Previous studies have suggested that miRNA-218 mediates the expression of developmentally sensitive genes (Chiavacci et al., 2012). In addition, it was found that miRNA-218 directly suppresses multiple transcription factors, one of which, HNF-6, is expressed within motor neurons and the brain (Guo et al., 2014; Landry et al., 1997; Simion et al., 2010). Based on this precedent, miRNA-218 may regulate Kif21b and Syt13 indirectly by acting on transcription mediators or factors that normally regulate Kif21b and Syt13 expression. To evaluate this, qPCR and sensor experiments should be carried out on conditions affecting transcription mediators that are predicted to be regulated by miRNA-218.

Canonical understanding of postnatal brain development suggests that it can be separated into two phases: an early phase where neural activity drives the pavement of a coarse network, and a later period where synapses are pruned to leave behind a refined neural network (Blankenship and Feller 2010). Animals injected with a.101.F showed increased neuronal activity levels within their hippocampus. NKCC1, one of the targets examined for miRNA-101, serves as a key chloride transporter that helps maintain excitatory GABA (Yamada et al., 2004). Its regulation may provide the explanation for the increased activity levels. Orderly decreased expression of NKCC1 helps brings about the GABA switch that establishes GABA as an inhibitory neurotransmitter in the mature brain (Yamada et al., 2004). It was also shown that animals deficient in NKCC1 have

reduced numbers of calcium events during early brain development (Pfeffer et al., 2009). Release of NKCC1 from miRNA-101 regulation can prolong excitatory GABA and likely produce the basis for the increased activity levels observed in animals treated with a.101.F

Dendritic growth and synapse formation are activity-dependent neural network features (Ben-Ari 2001). All three targets of miRNA-101 show involvement with these morphological characteristics. For NKCC1, premature switching of GABA has been implicated in producing underdeveloped dendrites (Cancedda et al., 2007), while Ank2 and Kif1a have been shown to have roles in synapse formation or stabilization (Bulat et al., 2014; Kondo et al., 2012). Consistent with these findings, animals injected with NKCC1-TSB showed much more complex dendritic arborization, and animals injected with both Kif1a and Ank2-TSBs exhibited increased glutamatergic synapses. These two findings indicate that miRNA-101 regulates multiple developmental programs to shape early coarse networks.

Using results obtained from the sensor and TSB experiments, we were able to verify that miRNA-101 directly targets NKCC1, Kif1a, and Ank2 to fine-tune the formation of proper neural networks. Our work sheds light on early brain development and suggests potential targets for further study from the perspective of developing treatments for diseases arising from excessive early network growth.

Appendix I: Acknowledgements

Giordano Lippi conducted Ca^{2+} imaging and analysis of miRNA-101 conditions (Figure S1). Seth R. Taylor conducted Ca^{2+} imaging for miRNA-136 and -218, and analysis for -218 conditions (Figure 1). MiRNA-101 qPCR experiments were done by Giordano Lippi, and -218 qPCR experiments by Yusuf Abacci (Figure S2). Giordano Lippi and I performed NKCC1, Kif1a, and Ank2 experiments. I independently performed the miRNA-218 sensor experiment.

Appendix II: Materials and Methods

Animals

Male C57Bl/6 (Harlan Laboratories) mice were used in all animal experiments. Animals were housed with their dams in a room that was maintained at 23 $\pm$ 1^{o}C with a 12/12 h light/dark cycle (07:00 AM – 07:00 PM). Free access to food and water was given to the animals. All procedures were conducted at the University of California at San Diego (UCSD), and performed as approved by the Institutional Animal Care and Use Committee and according to the National Institutes of Health Guidelines for the Care and Use of Laboratory Animals.

Calcium Imaging Analysis

Neuron activity was evaluated through analyzing videos of calcium transients of hippocampal neurons of P8 animals. Video frames capturing artifacts were removed. Clear videos were aligned using the ImageJ Stack plugin, then analyzed using a custom-made pipeline developed for Matlab (Frady et al., 2015 and 2016). Region of interests (ROIs) were drawn on neurons that exhibited less than 150 frames of continuous activity and possessed a clear KCl response. Two thresholds were drawn to capture calcium transient spikes and exclude data from the KCl response. Calcium transient spike thresholds were drawn through tracings that were 1.5 times greater than baseline, and the KCl threshold was drawn immediately prior to the onset of the KCl tracing.

Injections of LNAs and Viruses

All injections were performed under sterile conditions on P2 animals. P2 pups were placed on crushed ice that was covered by a sheet of Saran wrap. Crushed ice was used to anesthetize the animals via deep hypothermia and Saran wrap was used to prevent frost damage. Once animals became unresponsive, injections were made with a beveled glass injection pipette (Flared Glass: 4.45 cm long, 90 μm diameter) (Adesnik et al., 2008) attached to a Nanoject (Lozada et al., 2012) (Drummond Scientific Company, Broomall, PA). Two injections in each dorsal hippocampus were made at 1 mm below the skull. Three separate 69 nl injections were made at 10 sec intervals at each injection site. Post-surgery, the animals were cleaned of blood, placed on a heated pad to recover, and transferred back into their cages.

Using data from previous work (Hollander at al., 2010; Jimenez-Mateos et al., 2012; Zovoilis et al., 2011), the working concentrations for the LNAs and TSBs used were calculated based on miRNA abundance and volume of the dorsal hippocampus at P2. LNAs (Exiqon) had 0.5-1 μM concentrations and 165-333 nM for TSBs (Exiqon).

Antagonists:

a.Ctrl.F: gtgtaacacgtctatacgccca.

a.101.F: tcagctatcacagtact.

a.136.F: tcaaaacaaatggag.

a.218.F: ggttagatcaagcaca.

Target site blockers:

NKCC1-TSB: acagtacagtattatcaa.

Kif1a-TSB: cagacagtagggatgctg.

Ank2-TSB: tcacagtattcaagtttt.

Sensor Experiments

A Lentiviral miRNA-19 tracer (Han et al., 2016) was modified to create the miRNA-101 and -218 lentiviral sensors. The original tracer contained a constitutively expressed GFP driven by a miniCMV promoter, and RFP driven by a CAG promoter followed by miRNA-19 MREs. To provide room for RFP_{670} (ADDGENE) and its mutated or putative miRNA targets (IDT), restriction enzymes, BamHI and KpnI, were used to remove the original RFP and miRNA-19 MREs. Mutated and putative truncated 3'UTR target scripts were blasted against all known miRNAs (MiRBase) to ensure that MREs for other highly neuronally expressed miRNAs were not introduced, and subsequently introduced the tracer plasmid using AscI and KpnI. Completed sensor plasmids for miRNA-101 and -218 targets were packaged into lentiviruses as described (Boyden et al., 2005; Han et al., 2009).

Antagonists with the fluophore TYE-563 were used to avoid interference with the GFP channel. At P7, the animals were sedated with 0.05 ml of ketamine/xylazine anesthetic (10% ketamine, 1% xylazine, 0.9% NaCl). Sedated animals were perfused through the left ventricle with cold PBS followed by cold 4% paraformaldehyde (PFA) in PBS until their carcasses became rigid**.** The brains were then removed and postfixed overnight in 4% PFA in PBS solution.

Prior to sectioning, the brains were transferred to 30% sucrose in PBS for cryoprotection. Once the brains sunk, they were sectioned into 40 μm thick sections using a sliding microtome (Leica, SM210R). Slices were placed onto slides and coverslipped with Vectashield (Vector Laboratories).

Images of the slices were taken on a Leica SP5 laser scanning confocal microscope (at 2 μm steps using 20X oil immersion objective). The same acquisition settings (laser power, gain, offset) for GFP and RFP_{670} was used within each miRNA condition.

Maximum projections of z-stacks were used to acquire ROIs. ROIs were draw in the GFP channel using ImageJ, and average fluorescence intensity was measured in the GFP and RFP_{670} channels. The ratio of RFP_{670} to GFP were compared between mutated and putative MRE conditions. 1-5 animals were used for each condition.

*Kif1a Sensor:

WT: ttctcaGGCGCGC**C**ccaatgttcacagcatccc**TACTGT**ctggaaggtcatagaaggtcccga gtgttagctgtaggctcctg**TACTGT**ttgtgtgcacttagggctctgtGGTACCttctctctc

MUT: ttctcaGGCGCGCCccaatgttcacagcatccc**TCGTAC**ctggaaggtcatagaaggtcccg agtgttagctgtaggctcctg**TCGTAC**ttgtgtgcacttagggctctgtGGTACCttctctctc

*Ank2 sensor:

WT: gtgtacgtactttctcaGGCGCGCCtatcaaaaacttgaa**TACTGT**gagaagtgaattttcag ttccaaccttaagat**TACTGT**cagcataacaGGTACCttctcactactactactttcgtcgt

MUT: gtgtacgtactttctcaGGCGCGCCtatcaaaaacttgaa**TCGTAC**gagaagtgaattttcagt tccaaccttaagat**TCGTAC**cagcataacaGGTACCttctcactactactactttcgtcgt

*NKCC1 sensor:

WT: gtgtacgtactttctcaGGCGCGCCtgctaagtttgaaatgtaatattttgataa**TACTGTA**ctgttc ctgtgacagacgcctttgtaatgttttaaccctgagcGGTACCttctcactactactactttcgtcgt

MUT: gtgtacgtactttctcaGGCGCGCCtgctaagtttgaaatgtaatattttgataa**TCGTACA**ctgtt
cctgtgacagacgcctttgtaatgttttaaccctgagcGGTACCttctcactactactactttcgtcgt

*Kif21b sensor:

WT: atatgcGGCGCGCCgttggagtccctgctcacccacccttttcggggatgtccgattaacatagcttc
gggcaggaccccagctccactcattgcacaatgcgccttcttgtcgg**AAGCACAA**actggttgtaatcgt**A
GCACAA**gcaggcctggaatggtcttagtaaatgtggcttgggcaaagggcagctta**AAGCACAA**acc
cagactgcagggtctcgtttggctcatgcactctcctgtgacgtagt**AGCACAA**ggtgtgtatatgttttgtaaa
gttgctgacaactgtacatagtgtatgaaagttatttaagcctcatgcacgccattttggttctggaGGTACCata
tgc

Mut: atatgcGGCGCGCCgttggagtccctgctcacccacccttttcggggatgtccgattaacatagcttc
gggcaggaccccagctccactcattgcacaatgcgccttcttgtcgg**AACGTGAA**actggttgtaatcgt**G
CGTGAA**gcaggcctggaatggtcttagtaaatgtggcttgggcaaagggcagctta**AAGTCGGA**acc
cagactgcagggtctcgtttggctcatgcactctcctgtgacgtagt**AGACTTA**ggtgtgtatatgttttgtaaag
ttgctgacaactgtacatagtgtatgaaagttatttaagcctcatgcacgccattttggttctggaGGTACCatat
gc

*Syt13 sensor:

WT: atatgcGGCGCGCCgatgtaaaggggccccgggggaaggggcagtgtctggcctgaactgagg
tgggaatctttggaggagaaagttggtcctgtgcagtgtttctacccttgcgtgatcctgttgttagatgctgcgtgtac
cggatgccattccacataa**AAGCACAA**aaagtcgcatgagacatcgtggtcacatgtctggttacactttgg
AGCACAAaatcttacagtggtaaataaatcgttttccaatcgggttggcagcccagtgtttctctttgttcctttac
attaatattttagattgtcaaaattcagaaaGGTACCatatgc

Mut: atatgcGGCGCGCCgatgtaaaggggccccgggggaaggggcagtgtctggcctgaactgagg
tgggaatctttggaggagaaagttggtcctgtgcagtgtttctacccttgcgtgatcctgttgttagatgctgcgtgtac
cggatgccattccacataa**AGCGTCAA**aaagtcgcatgagacatcgtggtcacatgtctggttacactttgg
AGACTCAaatcttacagtggtaaataaatcgttttccaatcgggttggcagcccagtgtttctctttgttcctttac
attaatattttagattgtcaaaattcagaaaGGTACCatatgc

*Restriction sites in uppercase. MREs in bold.

VGlut1 Immunocytochemistry

Perfusions and brain sections were performed as described above for P15 animals. 40 µm thick brain sections were permeabilized and blocked at room temperature for 1 hour in PBS [pH 7.4, 0.3% Triton X-100 (PBST), 5% donkey serum (DS)]. After permeabilization and blocking, the primary antibodies were

applied to the sections overnight at 4°C in a solution containing 0.3% PBST, 5% DS, and the corresponding primary antibody (VGlut1, 1:500, AB5905 Millipore; GFAP, 1:1000, G3893 Sigma; Ki1a, 1:200, sc-19106 Santa Cruz Biotechnology; Ank2, 1:100, AB192769 Abcam). Three washes with PBS were made to the sections followed by incubation with secondary antibodies (donkey anti-guinea pig CF488A, 1:500, 20169-1 Biotium; donkey anti-mouse Alexa 488, 1:500, 49728A Invitrogen; donkey anti-goat Alexa 555, 1:500, A21432 Invitrogen; donkey anti-mouse Alexa 555, 1:500, A31570 Invitrogen). Finally, the slices were washed three times in PBS**,** stained with Draq5 (62254 ThermoFisher), and mounted with Vectashield.

Images were taken on a Leica SP5 laser scanning confocal microscope (at 2 μm steps using 20X oil immersion objective). The same acquisition settings (laser power, gain, offset) for GFP and RFP_{670} was used within all conditions.

Three optical sections localized close to the tissue surface of the striatum radiatum were merged and used per slice. Particle analysis was done using the ImageJ nucleus counter plugin (Size =10-300, watershed filter = ON). Two 16x16 μm images per slice and two slices per animal were used for analysis. 4-5 P15 animals, from 7 litters, were used for each condition.

Analysis of dendritic complexity and dendritic spines

Analysis of neurites was done at P8 and dendritic protrusions at P11. Glycoprotein-deleted variant of SAD-B19 strain of rabies encoding eGFP (SADΔG-eGFP) was employed to sparsely label CA1 and CA3 pyramidal

neurons (Ginger et al., 2013). Injections, perfusions, and brain extractions were followed as described above. To ensure intact dendritic structures, brains were sectioned coronally at 80 μm with a microtome (Leica). Confocal z-stacks of intact neurons were acquired with a Leica TCS SP5 microscope using a 20X lens and of spines using a 63X lens. Dendritic analysis was performed on ImageJ with the NeuronJ (Meijering et al., 2004) plugin to trace primary and secondary dendrites. Spines were separated into the classifications filopodia, thin, mushroom, and stubby, and separate counts were made for each in ImageJ. 3-6 animals, from 3 litters, were used for each condition.

Bibliography

Abelson, J.F., Kwan, K.Y., O'Roak, B.J., Baek, D.Y., Stillman, A.A., Morgan, T.M., Mathews, C.A., Pauls, D.L., Rasin, M.R., Gunel, M., Davis, N.R., Ercan-Sencicek, A.G., Guez, D.H., Spertus, J.A., Leckman, J.F., Dure, L.S. 4th., Kurlan, R., Singer, H.S., Gilbert, D.L., Farhi, A., Louvi, A., Lifton, R.P., Sestan, N., and State, M.W. (2005). Sequence variants in SLITRK1 are associated with Tourette's syndrome. Science 310, 317-320.

Adesnik, H., Li, G., During, M.J., Pleasure, S.J., and Nicoll, R.A. (2008). NMDA receptors inhibit synapse unsilencing during brain development. Proc Natl Acad Sci USA 105, 5597-5602.

Bartel, D.P. (2004). MicroRNAs: genomics, biogenesis, mechanism, and function. Cell 116, 281-297.

Bean, B.P. (2007). The action potential in mammalian central neurons. Nature Rev Neurosci 8, 451-465.

Ben-Ari, Y. (2001). Developing networks play a similar melody. Trends Neurosci 24, 353-360.

Ben-Ari, Y. (2002). Excitatory actions of gaba during development: the nature of the nurture. Nat Rev Neurosci 3, 728-739.

Bernstein E., Caudy A.A., Hammond S.M., and Hannon G.J. (2001). Role for a bidentate ribonuclease in the initiation step of RNA interference. Nature 409, 363-369.

Blankenship, A.G., and Feller, M.B. (2010). Mechanisms underlying spontaneous patterned activity in developing neural circuits. Nat Rev Neurosci 11, 18-29.

Boudreau, R.L., Jiang, P., Gilmore, B.L., Spengler, R.M., Tirabassi, R., Nelson, J.A., Ross, C.A., Xing, Y., and Davidson, B.L. (2014). Transcriptome-wide discovery of microRNA binding sites in human brain. Neuron 81, 294-305.

Boyden, E.S., Zhang, F., Bamberg, E., Nagel, G., and Deisseroth, K. (2005). Millisecond-timescale, genetically targeted optical control of neural activity. Nat Neurosci 8, 1263–1268.

Bulat, V., Rast, M., and Pielage, J. (2014). Presynaptic CK2 promotes synapse organization and stability by targeting Ankyrin2. J Cell Biol 204, 77-94.

Cancedda, L., Fiumelli, H., Chen, K., and Poo, M.M. (2007). Excitatory GABA action is essential for morphological maturation of cortical neurons in vivo. J Neurosci 27, 5224-5235.

Chen, Y., and Sabatini, B. L. (2012). Signaling in dendritic spines and spine microdomains. Current Opinion in Neurobiology 22, 389–396.

Chi, S.W., Zang, J.B., Mele, A., and Darnell, R.B. (2009). Argonaute HITS-CLIP decodes microRNA-mRNA interaction maps. Nature 460, 479-486.

Chiavacci, E., Dolfi, L., Verduci, L., Meghini, F., Gestri, G., Evangelista, A.M.M., Wilson S., Cremisi F., and Letizia Pitto. (2012). MicroRNA 218 Mediates the Effects of Tbx5a Over-Expression on Zebrafish Heart Development. PLoS ONE 7, e50536.

Crépel, V., Aronov, D., Jorquera, I., Represa., A., Ben-Ari, Y., and Cossart, R. (2007). A parturition-associated nonsynaptic coherent activity pattern in the developing hippocampus. Neuron 54, 105-120.

Cuellar, T.L., Davis, T.H., Nelson, P.T., Loeb, G.B., Harfe, B.D., Ullian, E., and McManus, M.T. (2008). Dicer loss in striatal neurons produces behavioral and neuroanatomical phenotypes in the absence of neurodegeneration. Proc Natl Acad Sci USA 105, 5614-5619.

Darnell, R.B. (2010). HITS-CLIP: panoramic views of protein-RNA regulation in living cells. Wiley Interdiscip Rev RNA 1, 266-286.

Davis T.H., Cuellar T.L., Koch S.M., Barker A.J., Harfe B.D., McManus M.T., and Ullian E.M. (2008). Conditional loss of Dicer disrupts cellular and tissue morphogenesis in the cortex and hippocampus. J Neurosci 28, 4322-4330.

Digilio, M.C., Marino, B., Capolino, R., and Dallapiccola, D. (2005). Clinical manifestations of deletion 22q11.2 syndrome (DiGeorge/Velo-Cardio-Facial syndrome). Paedoatr Cardiol 7, 23-34.

Duursma, A.M., Kedde, M., Schrier, M., le Sage, C., and Agami, R. (2008). miR-148 targets human DNMT3b protein coding region. RNA 14, 872-877.

Elton, T.S., Sansom S.E., and Martin M.M. (2010). Trisomy-21 gene dosage over-expression of miRNAs results in the haploinsufficiency of specific target proteins. RNA Biol 7, 540-547.

Frady, E.P., Kapoor, A., Horvitz, E., Kristan, W.B. (2016). Scalable semi-supervised functional neurocartography reveals canonical neurons in behavioral networks. Neural Comput 28, 1453-97.

Frady, E.P., Kristan, W.B. (2015). The Imaging Computational Microscope. arXiv:1502.07009.

Ginger, M., Haberl, M., Conzelmann, K.K., Schwarz, M.K., and Frick, A. (2013). Revealing the secrets of neuronal circuits with recombinant rabies virus technology. Front Neural Circuits 7, 2.

Gregory, R.I., Chendrimada, T.P., Cooch N., and Shiekhattar, R. (2005). Human RISC couples MicroRNA biogenesis and posttrancriptional gene silencing. Cell 4, 63-640.

Guo, J., Zhang, J.F., Wang, W.M., Cheung, F.W., Lu, Y.F., Ng, C.F., Kung, H.F., and Liu, W.K. (2014). MicroRNA-218 inhibits melanogenesis by directly suppressing microphthalmia-associated transcription factor expression. RNA Biol 11, 732-741.

Han, J., Kim, H.J., Schafer, S.T., Paquola, A., Clemenson, G.D., Toda, T., Oh, J., Pankonin, A.R., Lee, B.S., Johnston, S.T., Sarkar, A., Denli, A.M., and Gage, F.H. (2016). Functional Implications of miR-19 in the Migration of Newborn Neurons in the Adult Brain. Neuron 91, 79-89.

Han J., Lee Y., Yeom K.H., Kim Y.K., Jin H., and Kim V.N. (2004). The Drosha-DGCR8 complex in primary microRNA processing. Genes Dev 18, 3016-3027.

Han, X., Qian, X., Bernstein, J.G., Zhou, H.H., Franzesi, G.T., Stern, P., Bronson, R.T., Graybiel, A.M., Desimone, R., and Boyden, E.S. (2009). Millisecondtimescale optical control of neural dynamics in the nonhuman primate brain. Neuron 62, 191–198.

Hering, H., and Sheng, M. (2001). Dendritic spines: structure, dynamics and regulation. Nat Rev Neurosci 2, 880-888.

Hirokawa, N., Noda, Y., Tanaka, Y., and Niwa, S. (2009). Kinesin superfamily motor proteins and intracellular transport. Nat Rev Mol Cell Biol 10, 682-696.

Hollander, J.A., Im, H.I., Amelio, A.L., Kocerha, J., Bali, P., Lu, Q., Willoughby, D., Wahlestedt, C., Conkright, M.D., and Kenny, P.J. (2010). Striatal microRNA controls cocaine intake through CREB signalling. Nature 466, 197-202.

Huntzinger, E., and Izaurralde El. (2011). Gene silencing by microRNAs: contributions of translational repression and mRNA decay. Nature Reviews Genetics 12, 99-110.

Iwakawa, H., and Tomari, Y. (2015). The functions of MicroRNAs: mRNA decay and translational repression. Trends in Cell Biology 11, 651-665.

Jimenez-Mateos, E.M., Engel, T., Merino-Serrais, P., McKiernan, R.C., Tanaka, K., Mouri, G., Sano, T., O'Tuathaigh, C., Waddington, J.L., Prenter, S., Delanty Norman., Farrell M., O'Brien D., Conroy R., Stallings R., DeFelipe J., and David Hensall. (2012). Silencing microRNA-134 produces neuroprotective and prolonged seizure-suppressive effects. Nat Med 18, 1087-1094.

Jin, P., Zarnescu D.C., Ceman S., Nakamoto M., Mowrey, J., Jongens, T.A., Nelson, D.L., Moses K., and Warren S.T. (2004). Biochemical and genetic interaction between the fragile X mental retardation protein and the microRNA pathway. Nat Neurosci 7, 113-117.

Kanjhan, R., Noakes, P.G., and Bellingham, M.C. (2016). Emerging Roles of Filopodia and Dendritic Spines in Motoneuron Plasticity during Development and Disease. Neural Plasticity 2016, 31.

Katz, L.C., and Shatz, C.J. (1996). Synaptic activity and the construction of cortical circuits. Science 274, 1133-1138.

Kawamata, T., and Tomari, Y. (2010). Making RISC. Trends in Biochem Sci 7, 368-376.

Knight S.W., and Bass B.L. (2001). A role for the RNase III enzyme DCR-1 in RNA interference and germ line development in Caenorhabditis elegans. Science 293, 2269-2271.

Kondo, M., Takei, Y., and Hirokawa, N. (2012). Motor protein KIF1A is essential for hippocampal synaptogenesis and learning enhancement in an enriched environment. Neuron 73, 743-757.

Kuhn D.E., Nuovo G.J., Terry A.V., Martin M.M., Malana G.E., Sansom S.E., Pleister A.P., Beck W.D., Head E., Feldman D.S., and Elton T.S. (2010). Chromosome 21-derived microRNAs provide an etiological basis for aberrant protein expression in human Down syndrome brains. J Biol Chem 285, 1529-1543.

Landrya, C.,Clotmanb, F., Hiokic, T., Odac, Hiroaki., Picardb, J.J., Lemaigrea, F.P., and Rousseaua, G.G. (1997). HNF-6 is expressed in endoderm derivatives and nervous system of the mouse embryo and participates to the cross-regulatory network of liver-enriched transcription factor. Developmental Biology 192, 247-257.

Lee Y., Ahn, C., Han, J., Choi, H., Kim, J., Yim, J., Lee, J., Provost, P., Radmark, O., Kim, S., and Kim V.N. (2003). The nuclear RNase III drosha initiates microRNA processing. Nature 425, 415-419.

Lee Y., Jeon K., Lee J.T., Kim S., and Kim V.N. (2002). MicroRNA maturation: stepwise processing and subcellular localization. EMBO J 21, 4663-4670.

Leinekugel, X., Khazipov, R., Cannon, R., Hirase, H., Ben-Ari, Y., and Buzsáki G. (2002). Correlated bursts of activity in the neonatal hippocampus in vivo. Science 297. 2049-2052.

Lippi, G., Fernandes, C. C., Ewell, L. A., John, D., Romoli, B., Curia, G., et al., (2016). MicroRNA-101 Regulates Multiple Developmental Programs to Constrain Excitation in Adult Neural Networks. Neuron, 92, 1337-1351.

Lippi, G., Steinert, J.R., Marczylo, E.L., D'Oro, S., Fiore, R., Forsythe, I.D., Schratt, G., Zoli, M., Nicotera, P., and Young, K.W. (2011). Targeting of the Arpc3 actin nucleation factor by miR-29a/b regulates dendritic spine morphology. J Cell Biol 194, 889-904.

Lozada, A.F., Wang, X., Gounko, N.V., Massey, K.A., Duan, J., Liu, Z., and Berg, D.K. (2012). Glutamatergic synapse formation is promoted by alpha7-containing nicotinic acetylcholine receptors. J Neurosci 32, 7651-7661.

Meijering, E., Jacob, M., Sarria, J.C., Steiner, P., Hirling, H., and Unser, M. (2004). Design and validation of a tool for neurite tracing and analysis in fluorescence microscopy images. Cytometry A 58:167–176.

Minju H., and Kim V.N. (2014). Regulation of microRNA biogenesis. Nature Rev Mol Cell Biology 15, 509-524.

Mohler, J.P., Anthony, O., and Vann Bennett, G. (2002). Ankyrins. Journal of Cell Science 115, 1565-1566.

Paredes, R.M., Etzler, J.C., Watts, L.T., and Lechleiter, J.D. (2008). Chemical Calcium Indicators. Methods 46, 143-151.

Park J.E., Heo I., Tian Y., Simanshu D.K., Chang H., Jee D., Patel D.J., and Kim V.N. (2011). Dicer recognizes the 5' end of RNA for efficient and accurate processing. Nature 475, 201-205.

Pfeffer, C.K., Stein, V., Keating, D.J., Maier, H., Rinke, I., Rudhard, Y., Hentschke, M., Rune, G.M., Jentsch, T.J., and Hübner, C.A. (2009). NKCC1-dependent GABAergic excitation drives synaptic network maturation during early hippocampal development. J Neurosci 29, 3419-3430.

Rivera, C., Voipio, J., Payne, J.A., Ruusuvuori, E., Lahtinen, H., Lamsa, K., Pirvola, U., Saarma, M., and Kaila, K. (1999). The K+/Cl- co-transporter KCC2 renders GABA hyperpolarizing during neuronal maturation. Nature 397, 251-255.

Rajasethupathy P., Fiumara F., Sheridan R., Betel B., Puthanveettil V. S., Russo R., Sander C., Tuschl T., and Eric Kandel (2009). Characterization of small RNAs in aplysia reveals a role for miR-124 in constraining synaptic plasticity through CREB. Neuron 63, 803–817.

Simion, A., Laudadio, I., Prévot, P.P., Raynaud, P., Lemaigre, F.P., Jacquemin, P. (2010). MiR-495 and miR-218 regulate the expression of the Onecut transcription factors HNF-6 and OC-2. Biochem Biophys Res Commun 391, 293-298.

Smrt, Richard D., Keith E. Szulwach, Rebecca L. Pfeiffer, Xuekun Li, Weixiang Guo, Manavendra Pathania, Zhao-Qian Teng, Yuping Luo, Junmin Peng, Angelique Bordey, Peng Jin, and Xinyu Zhao. MicroRNA miR-137 regulates neuronal maturation by targeting ubiquitin ligase Mind Bomb-1. Stem Cells 28, 1060-1070.

Takamori, S., Holt M., Katinka S., Lemnke E., Gronbord M., Riedel D., Urlaub H., Schenk S., Brugger B., Ringler P., Muller S., Rammner B., Grater F., Hub j., Groot B., Mieskes G., Moriyama Y., Klingauf F., Grubmuller H., Heuser J., Wieland F., and Reinhard Jahn. (2006). Molecular Anatomy of a Trafficking Organelle. Cell 127, 831-846.

Tang, X., Zhang, Y., Tucker, L., and Ramratnam, B. (2010). Phosphorylation of the RNase III enzyme Drosha at Serine300 or Serine302 is required for its nuclear localization. Nucleic Acids Res 38, 6610-6619.

Tsutsumi A., Kawamata T., Izumi N., Seitz H., and Tomari Y. (2011). Recognition of the pre-miRNA structure by Drosophila Dicer-1. Nat Struct Mol Biol 18, 1153-1158.

Tyzio, R., Cossart, R., Khalilov, I., Minlebaev, M., Hübner, C.A., Represa, A., Ben-Ari, Y., and Khazipov, R. (2006). Maternal oxytocin triggers a transient inhibitory switch in GABA signaling in the fetal brain during delivery. Science 314, 1788-1792.

Winter, J., Jung, S., Keller, S., Gregory, R.I., and Diederichs, S. (2009). Many roads to maturity: microRNA biogenesis pathways and their regulation. Nature Cell Biology 11, 228-234.

Wu H., Xu H., Miraglia L.J., and Crooke S.T. (2000) Human RNase III Is a 160-kDa protein involved in preribosomal RNA processing. J Biol Chem 275, 36957-36965.

Yamada, J., Okabe, A., Toyoda, H., Kilb, W., Luhmann, H.J, and Fukuda, A. (2004). Cl- uptake promoting depolarizing GABA actions in immature rat neocortical neurones is mediated by NKCC1. J Physiol 557, 829-841.

Yekta, S., Shih, I.H., and Bartel, D.P. (2004). MicroRNA-directed cleavage of HOXB8 mRNA. Science 304, 594-596.

Yoko, K.K., Gaizka, O., and Tao S. (2009). Different timings of Dicer deletion affect neurogenesis and gliogenesis in the developing mouse central nervous system. Dev Dyn 238, 2800-2812.

Zhang H., Kolb F.A., Jaskiewicz L., Westhof E., and Filipowicz W. (2004). Single processing center models for human Dicer and bacterial RNase III. Cell 118, 57-68.

Zovoilis, A., Agbemenyah, H.Y., Agis-Balboa, R.C., Stilling, R.M., Edbauer, D., Rao, P., Farinelli, L., Delalle, I., Schmitt, A., Falkai, P., Bahari-Javan S., Burkhardt S., Sananbenesi F., and Andre Fischer. (2011). microRNA-34c is a novel target to treat dementias. EMBO J 30, 4299-4308.